

Document downloaded from:

<http://hdl.handle.net/10251/163986>

This paper must be cited as:

Vega-Moreno, J.; Lemus-Santana, A.; Reguera, E.; Andrio, A.; Compañ Moreno, V. (2020). High proton conductivity at low and moderate temperature in a simple family of Prussian blue analogs, divalent transition metal hexacyanocobaltates (III). *Electrochimica Acta*. 360:1-11. <https://doi.org/10.1016/j.electacta.2020.136959>



The final publication is available at

<https://doi.org/10.1016/j.electacta.2020.136959>

Copyright Elsevier

Additional Information

Supporting Information

High proton conductivity at low and moderate temperature in a simple family of Prussian blue analogs, transition metal hexacyanocobaltates (III)

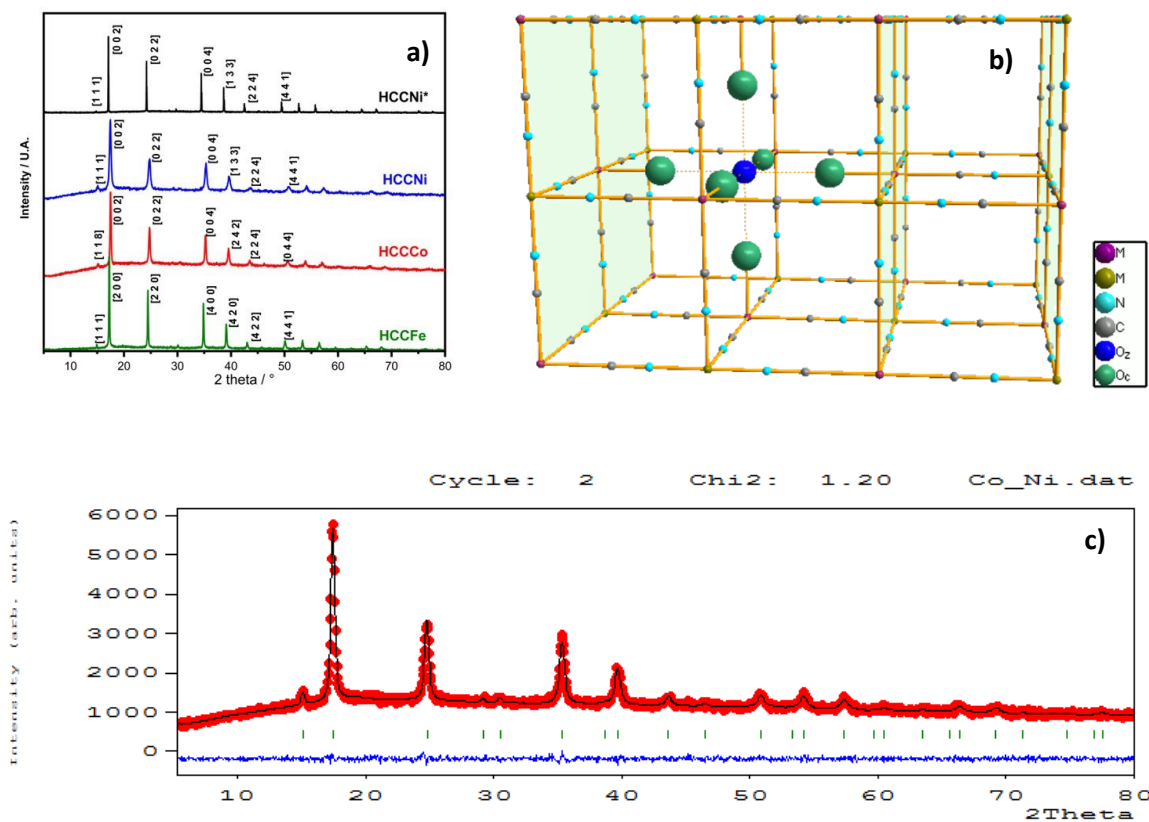
J. Vega^{1,2}, A. Andrio³, A. A. Lemus-Santana², E. Reguera², V. Compañ⁴

¹ CONACyT-Instituto Politécnico Nacional, Centro de Investigación en Ciencia Aplicada y Tecnología Avanzada, Legaria 694, Irrigación, Miguel Hidalgo, CDMX, México

² Centro de Investigación en Ciencia Aplicada y Tecnología Avanzada. Unidad Legaría. Instituto Politécnico Nacional. Legaria Núm. 694, Col. Irrigación, Miguel Hidalgo, C.P. 11500 Cd. México

³ Departamento de Física aplicada. Universitat Jaume I- 12080, Castellón (Spain)

⁴ Departamento de Termodinámica Aplicada. Escuela Técnica Superior de Ingenieros Industriales (ETSII). Universidad Politécnica de Valencia, Campus de Vera s/n, 46020- Valencia, Spain.



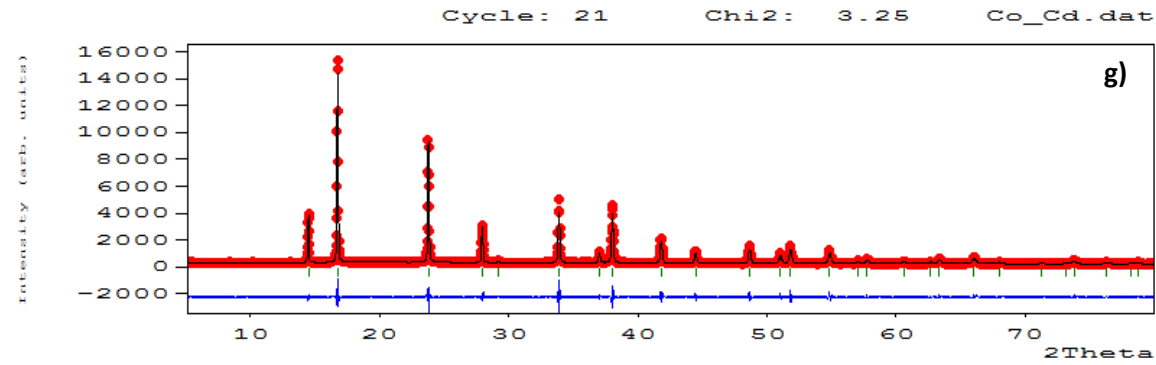
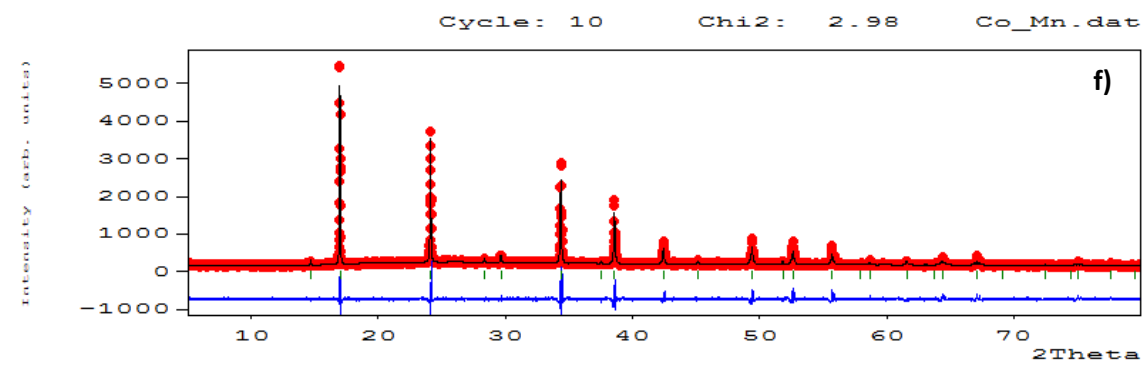
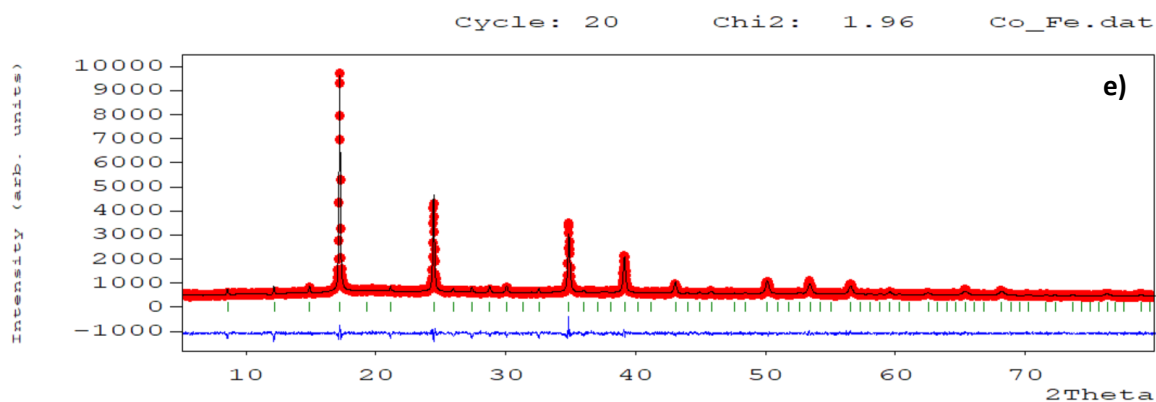
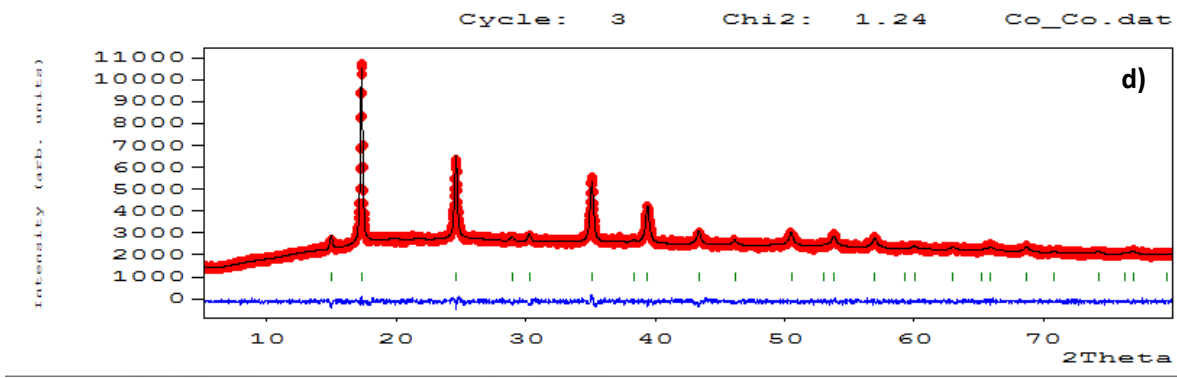


Figure 1S. a) PXRD patterns of HCCMs and nickel hexacyanocobaltate reported, b) Framework of the $M_3[Co(CN)_6]_2 \cdot xH_2O$ series for the members that crystallize within a Fm-3m space group (dehydrated at 65°C). Indicated are the coordinated and hydrogen bonded water molecules and fit Rietveld refined method to b) HCCNi, c) HCCC_o, d) HCCFe, e) HCCMn, and f) HCCCd.

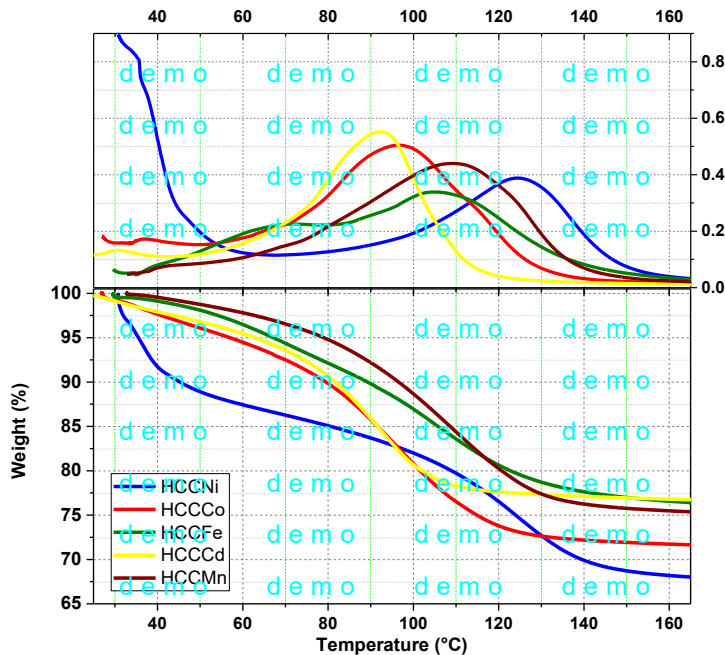


Figure 2S. TGA and DTG for HCCMs family in the low temperature region

Impedance spectroscopy measurements were carried out on the HCCMs family (HCCNi, HCCC_o, HCCFe, HCCMn and HCCCd). The data collection was made in the 25 - 115°C temperature range and within the frequency window of $10^{-1} < f < 3 \times 10^7$ Hz in the indicated humidity level in order to obtain the conductivity and diffusivity of the ionic charge carriers. The experiments were performed with a 100mV amplitude using a Novocontrol broadband dielectric spectrometer (Hundsangen, Germany) integrated with an SR 830 lock-in amplifier with an Alpha dielectric interface. The sample of interest was sandwiched between two circular gold electrodes coupled to the impedance spectrometer, which acted as blocking electrodes. The samples were stored in deionized water and subsequently sandwiched between the electrodes. During the measurements, the electrodes were kept in a BDS 1308 liquid device, which was coupled to the spectrometer and incorporated with deionized water

to ensure that the sample was fully-hydrated below 100°C and in equilibrium with its vapor above 105°C, to simulate 100% RH atmosphere. For the isothermal experiments, the temperature was controlled by a nitrogen jet (QUATRO from Novocontrol) with a temperature error of 0.1 K during every individual sweep in frequency.

The experimental data obtained from the powders samples were analyzed in terms of the complex dielectric permittivity function, $\varepsilon^*(\omega, T)$, and the complex conductivity $\sigma^*(\omega, T) = j\omega \varepsilon_0 \varepsilon^*(\omega, T)$ where j is the imaginary unity, ε_0 is the vacuum permittivity and ω the angular frequency of the applied electric field ($\omega=2\pi f$). Proton conductivity is generally measured along the plane of the sample in pill form. However, in practice, it requires proton conduction through plane perpendicular to the membrane. In this regard, electrochemical impedance spectroscopy (EIS), is the technique more appropriate to measure the through-plane conductivity of polymer electrolyte membranes to be applied in batteries, supercapacitors and fuel cells.

Table 1S. Frequency values of the onset (f_{ON}) and full development of electrode polarization (f_{MAX}). Static permittivity obtained experimentally and from eq. (17), respectively. Also in columns six, seven and eight we show the dc-conductivity and frequency values obtained at electrode polarization (f_{EP}) and cut-off frequency (f_c) considered as the frequency where the ac-conductivity is determined. In the last column the ionic charge density obtained following eq. (15) is also given.

HCCNi							
T (°C)	F _{MAXX} x 10 ⁻³ (Hz)	F _{ON} x 10 ⁻⁵ (Hz)	ε _s Theore- tical	ε _s Experi- mental	σ _{dc} x 10 ³ (S cm ⁻¹)	f _c x 10 ⁻⁵ (Hz)	D x 10 ⁶ (cm ² s ⁻¹)
25	2.65	8.25	48.09	47.98	6.87	15.7	0.43
35	3.57	11.19	43.75	43.61	8.55	15.8	0.13
45	4.99	16.65	35.21	35.48	10.71	15.9	0.06
55	6.94	28.51	20.06	20.14	13.10	21.1	0.08
65	9.38	37.11	17.45	17.58	14.25	23.1	0.85
75	11.1	48.21	11.38	11.23	13.29	25.1	20.36
85	10.9	26.62	27.28	27.27	9.88	27.1	25.05
95	8.69	17.79	32.70	32.51	6.63	35.8	26.44
105	6.71	13.39	33.23	33.27	4.94	39.8	-

25	0.39	0.47	97.4	97.68	0.31	3.98	0.10
35	0.45	0.59	97.3	96.34	0.41	6.56	0.15
45	0.71	0.84	96.1	96.31	0.53	10.0	0.26
55	1.00	1.12	95.0	95.48	0.70	11.8	0.45
65	1.29	1.41	94.8	94.70	0.82	12.2	0.75
75	1.34	1.59	92.3	91.96	0.96	13.9	1.40
85	2.14	2.15	94.8	91.30	1.14	14.3	2.23
95	6.15	4.91	94.3	99.31	2.06	19.8	4.68
105	3.37	6.39	83.6	83.56	5.63	-	-
HCCFe							
25	1.27	3.47	55.2	55.0	2.92	15.9	0.60
35	1.37	3.91	62.6	62.6	3.89	22.1	0.80
45	1.67	4.51	74.2	74.3	5.04	25.1	1.25
55	1.81	5.02	81.7	81.4	6.32	25.5	3.97
65	6.51	9.84	92.2	92.2	7.63	28.2	5.97
75	7.11	1.02	108.1	108.6	8.87	34.2	26.31
85	6.21	9.31	128.5	128.1	9.98	37.6	34.58
95	5.21	8.77	136.5	136.4	11.21	39.8	44.70
105	4.32	8.00	-	-	12.25	39.9	-
HCCMn							
25	1.01	1.17	43.63	43.76	0.02	0.10	0.95
35	1.11	1.30	45.40	45.21	0.03	0.19	1.37
45	1.22	1.49	45.89	46.93	0.04	0.12	1.64
55	1.30	1.58	49.27	49.02	0.05	0.15	1.72
65	2.52	2.28	51.85	51.03	0.05	0.16	2.54
75	4.13	2.90	54.72	54.93	0.06	0.19	4.64
85	7.13	3.97	58.79	58.53	0.07	0.20	9.89
95	9.65	5.00	61.70	61.68	0.08	0.25	32.2
105	1.35	5.95	65.34	65.28	0.09	0.39	-
HCCCd							
25	1.69	2.48	48.10	48.05	0.10	0.63	0.41
35	1.75	2.83	47.85	47.93	1.22	1.00	0.50
45	1.90	3.09	45.55	45.42	1.27	1.48	0.51
55	2.05	3.43	43.52	43.41	1.39	1.62	0.55
65	2.85	3.51	69.45	43.36	1.66	1.88	0.73
75	3.23	5.03	43.58	43.20	1.90	2.11	0.91
85	3.54	5.67	43.53	43.25	2.20	2.41	1.20
95	3.65	6.18	43.56	43.57	2.54	3.81	1.28
105	3.68	7.42	43.87	43.87	2.95	4.08	-

Table 2S. Charge mobility (μ) of HCCMs (in $\mu/\text{m}^2 \text{ V}^{-1}\text{s}^{-1}$)

Charge Mobility					
T / °C	HCCNi	HCCC _o	HCCFe	HCCCd	HCCMn

25	0.17	0.04	0.24	0.16	0.37
35	0.05	0.06	0.30	0.19	0.44
45	0.02	0.10	0.46	0.19	0.50
55	0.03	0.16	1.41	0.20	0.58
65	0.29	0.26	2.05	0.25	0.56
75	6.79	0.47	8.77	0.30	0.85
85	8.12	0.73	11.21	0.39	1.50
95	8.34	1.48	14.10	0.40	3.12
105	9.31	-	-	0.29	9.88

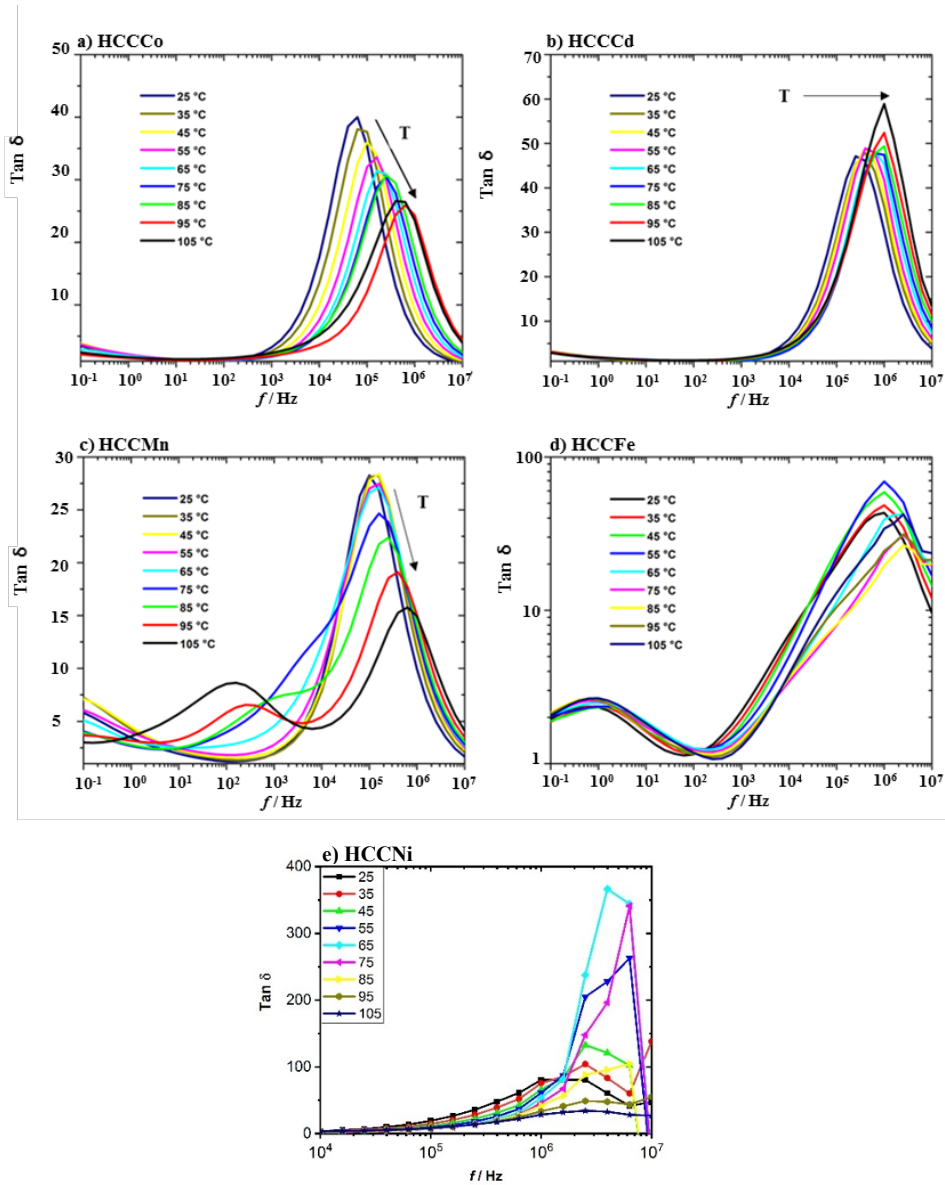


Figure 3S. Tan δ vs frequency in all the range of temperatures measured for some of samples studied, a) HCCC_o, b) HCCC_d, c) HCCMn and d) HCCFe.

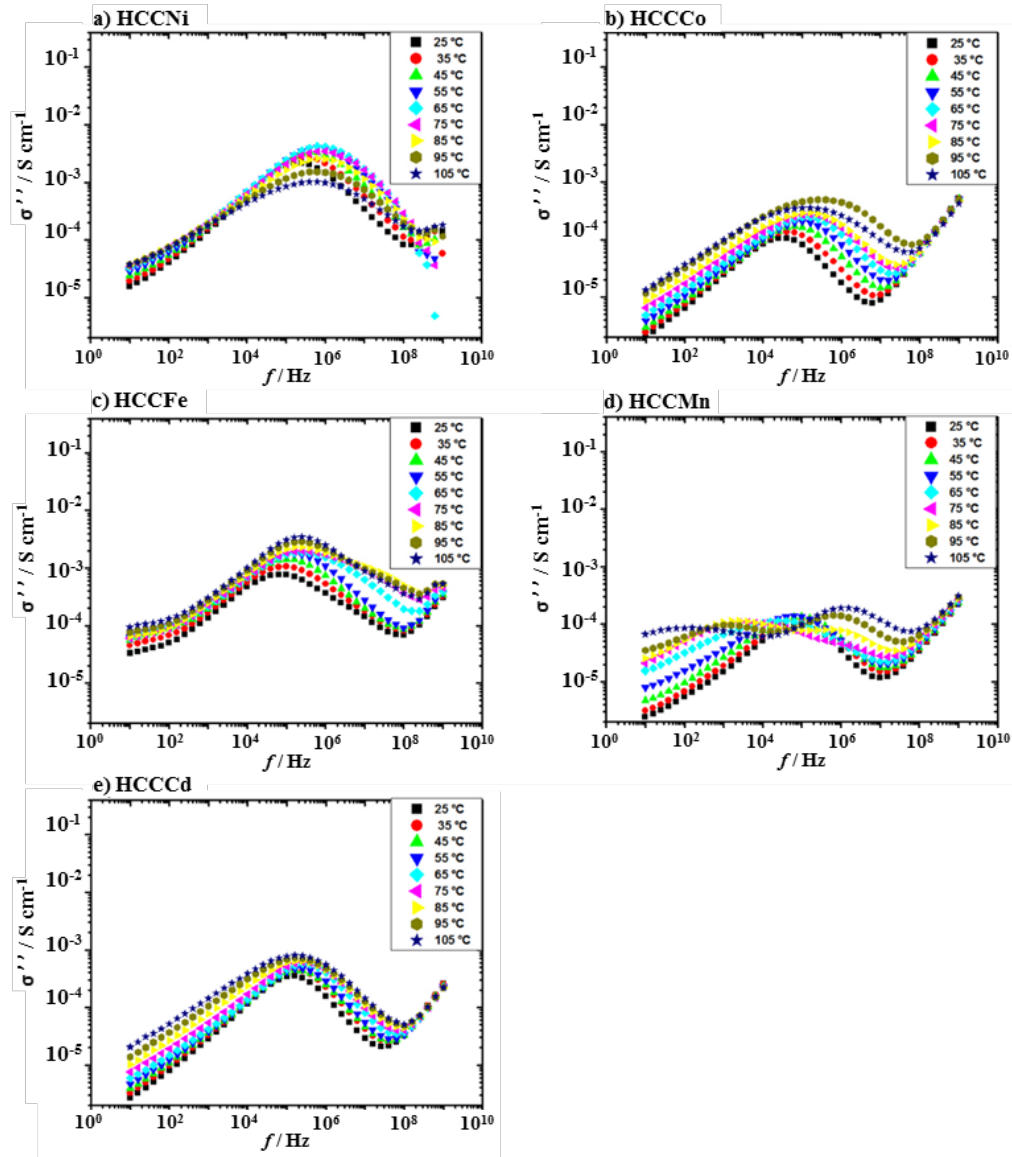


Figure 4S. Double logarithmic plot of the imaginary part of the conductivity vs. frequency for the samples HCCNi, HCCC_o, HCCC_d, HCCMn and HCCFe, respectively.

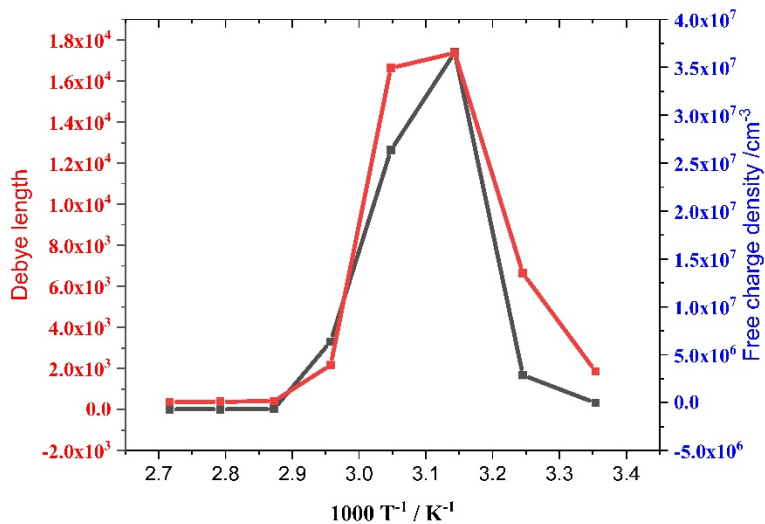


Figure 5S. Temperature dependence of Debye length and free charge density to HCCNi.

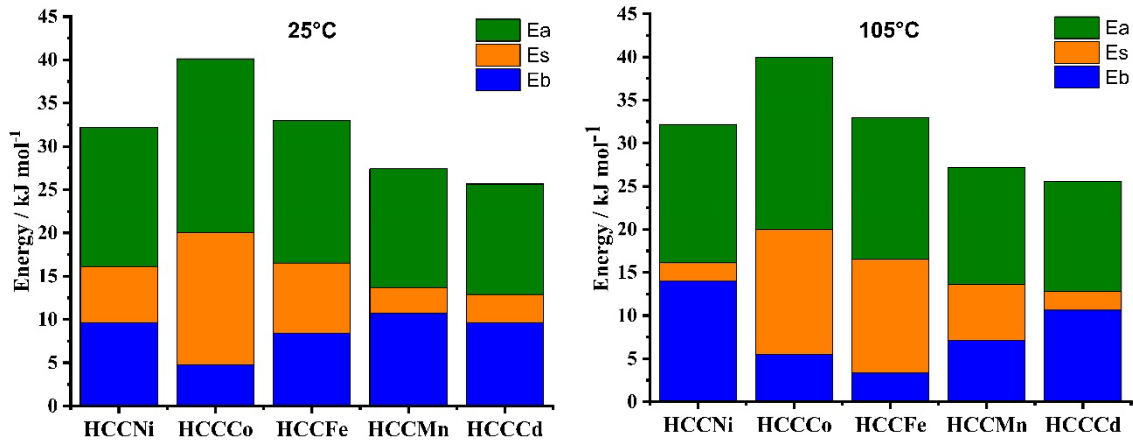


Figure 6S. Binding energy (Eb), stabilization energy (Es) and activation energy (Ea) for the series of HCCM materials at 25 and 105°C.

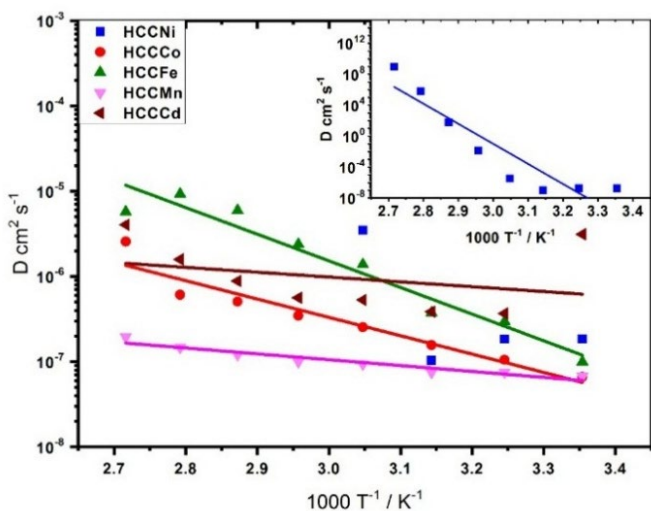


Figure 7S. Temperature dependence of diffusion coefficient obtained from Debye model.